The unconditionally stable semi-implicit ALE finite element scheme for fluid-structure interaction

Alexander Lozovskiy[1] **Yuri Vassilevski**[1,2]
Maxim Olshanskii[3] **Victoria Salamatova**[1,2]

[1]Institute of Numerical Mathematics RAS
[2]Moscow Institute of Physics and Technology
[3]University of Houston

The 8th Workshop on Mathematical Models and Numerical Methods in Biology and Medicine

October 31, 2016, Moscow

Intro and motivation

- This work has been conducted in active collaboration with Prof. M. Olshanskii (University of Houston), Prof. Y. Vassilevski, V. Salamatova (Institute of Numerical Mathematics of Russian Academy of Sciences) and was supported by the Russian Science Foundation (RSF) grant 14-31-00024

Intro and motivation

- This work has been conducted in active collaboration with Prof. M. Olshanskii (University of Houston), Prof. Y. Vassilevski, V. Salamatova (Institute of Numerical Mathematics of Russian Academy of Sciences) and was supported by the Russian Science Foundation (RSF) grant 14-31-00024
- Understanding fluid-structure interaction is important in many fields of engineering, such as design of aircraft, bridges, etc. Rigid body models may not be adequate in applications where sensitivity to oscillations is crucial.

Intro and motivation

- This work has been conducted in active collaboration with Prof. M. Olshanskii (University of Houston), Prof. Y. Vassilevski, V. Salamatova (Institute of Numerical Mathematics of Russian Academy of Sciences) and was supported by the Russian Science Foundation (RSF) grant 14-31-00024
- Understanding fluid-structure interaction is important in many fields of engineering, such as design of aircraft, bridges, etc. Rigid body models may not be adequate in applications where sensitivity to oscillations is crucial.
- Widely used as a base paradigm for the cardiovascular blood flow numerical studies in physiology and medicine.

Intro and motivation

- This work has been conducted in active collaboration with Prof. M. Olshanskii (University of Houston), Prof. Y. Vassilevski, V. Salamatova (Institute of Numerical Mathematics of Russian Academy of Sciences) and was supported by the Russian Science Foundation (RSF) grant 14-31-00024
- Understanding fluid-structure interaction is important in many fields of engineering, such as design of aircraft, bridges, etc. Rigid body models may not be adequate in applications where sensitivity to oscillations is crucial.
- Widely used as a base paradigm for the cardiovascular blood flow numerical studies in physiology and medicine.
- Challenges: treatment of boundary conditions at the interface, mixed parabolic-hyperbolic nature, coupling of equations, cost considerations.

Intro and motivation

- This work has been conducted in active collaboration with Prof. M. Olshanskii (University of Houston), Prof. Y. Vassilevski, V. Salamatova (Institute of Numerical Mathematics of Russian Academy of Sciences) and was supported by the Russian Science Foundation (RSF) grant 14-31-00024
- Understanding fluid-structure interaction is important in many fields of engineering, such as design of aircraft, bridges, etc. Rigid body models may not be adequate in applications where sensitivity to oscillations is crucial.
- Widely used as a base paradigm for the cardiovascular blood flow numerical studies in physiology and medicine.
- Challenges: treatment of boundary conditions at the interface, mixed parabolic-hyperbolic nature, coupling of equations, cost considerations.
- We use monolithic approach (fluid $+$ solid $=$ one domain)

Intro and motivation

Known simplifications:

- 1D FSI simulation with given dependence of the radii of the vessel on the blood pressure
- 3D Navier-Stokes within rigid walls
- 3D FSI with linear materials

Intro and motivation

Known simplifications:

- 1D FSI simulation with given dependence of the radii of the vessel on the blood pressure
- 3D Navier-Stokes within rigid walls
- 3D FSI with linear materials

Real caridovascular flow is 3D and the vessel walls are nonlinear!
Costly...

Intro and motivation

Known simplifications:

- 1D FSI simulation with given dependence of the radii of the vessel on the blood pressure
- 3D Navier-Stokes within rigid walls
- 3D FSI with linear materials

Real caridovascular flow is 3D and the vessel walls are nonlinear!
Costly...
Our method is semi-implicit and unconditionally stable $\rightarrow$ no Newton, no severe restriction on time-step.

Some relevant literature

- Aribtrary Lagrange-Euler monlolithic scheme:
  S. Turek, J. Hron, M. Madlik, M. Razzaq, H. Wobker, J. Acker, Numerical simulation and benchmarking of a monolithic multigrid solver for fluid-structure interaction problems with application to hemodynamics, Springer, Berlin, Heidelberg (2011)
- Partitioned schemes:
  G. Hou, J. Wang, A. Layton, Numerical methods for fluid-structure interaction - a review, Commun. Comput. Phys. 12 (2) (2012)
- FSI for blood flow:
  P. Crosetto, P. Reymond, S. Deparis, D. Kontaxakis, N. Stergiopulos, A. Quarteroni, Fluid-structure interaction simulation of aortic blood flow, Comput. & Fluids 43 (1) (2011)
- Constitutive models of blood vessel walls:
  R.P. Vito, S.A. Dixon, Blood vessel constitutive models-1995-2002, Ann. Rev. Biomed. Eng. 5 (1) (2003)
  Z. Yosibash, I. Manor, I. Gilad, U. Willentz, Experimental evidence of the compressibility of arteries, J. Mech. Behav. Biomed. Mater. 39 (2014)

  Z. Yosibash, E. Priel, p-FEMs for hyperelastic anisotropic nearly incompressible materials under finite deformations with applications to arteries simulation, Internat. J. Numer. Methods Engrg. 88 (11) (2011) 11521174.
- Mesh-moving operators:
  Wick T. Fluid-structure interactions using different mesh motion techniques, Comput. & Structures. 89(13) (2011)

FSI problem

Prerequisites

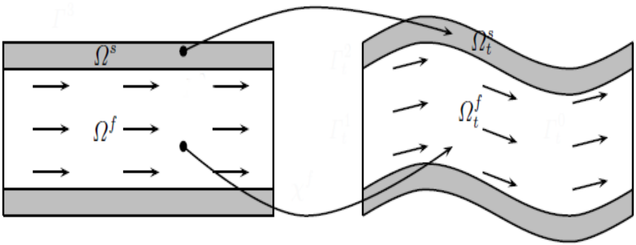

Meshing is performed in the left (initial) domain with coordinates $\mathbf{X}$, while the right (current) domain is described as $\mathbf{x} = \mathbf{x}(\mathbf{X}, t)$. Notation:

$$\mathbf{u} = \mathbf{x} - \mathbf{X}(\text{displacement}), \quad \mathbf{F} = \mathbf{I} + \nabla \mathbf{u}, \quad J = \det(\mathbf{F}), \quad \mathbf{E} = \frac{1}{2}(\mathbf{F}^T\mathbf{F} - \mathbf{I}).$$

$$\{\mathbf{A}\}_s = \frac{1}{2}(\mathbf{A} + \mathbf{A}^T) \quad \text{(symmetric part of tensor } \mathbf{A}\text{)}$$

Image taken from Hron J., Turek S. A monolithic FEM/multigrid solver for an ALE formulation of fluid-structure interaction with applications in biomechanics (2006).

FSI problem

Governing equations in reference subdomains

The kinematic and dynamic equations for the fluid and structure in the reference domains:

$$\frac{\partial \mathbf{u}}{\partial t} = \mathbf{v} \quad \text{in } \Omega_s,$$

$$\mathbf{G}\left(\mathbf{u}, \frac{\partial \mathbf{u}}{\partial t}\right) = 0 \quad \text{in } \Omega_f \quad \text{(extension of displacement)},$$

$$\frac{\partial \mathbf{v}}{\partial t} = \begin{cases} \rho_s^{-1} \mathrm{div}\left(J \boldsymbol{\sigma}_s \mathbf{F}^{-T}\right) & \text{in } \Omega_s, \\ (J\rho_f)^{-1} \mathrm{div}\left(J \boldsymbol{\sigma}_f \mathbf{F}^{-T}\right) - (\nabla \mathbf{v})\mathbf{F}^{-1}(\mathbf{v} - \frac{\partial \mathbf{u}}{\partial t}) & \text{in } \Omega_f. \end{cases} \tag{1}$$

FSI problem

Governing equations in reference subdomains

The kinematic and dynamic equations for the fluid and structure in the reference domains:

$$\frac{\partial \mathbf{u}}{\partial t} = \mathbf{v} \quad \text{in } \Omega_s,$$

$$\mathbf{G}\left(\mathbf{u}, \frac{\partial \mathbf{u}}{\partial t}\right) = 0 \quad \text{in } \Omega_f \quad \text{(extension of displacement)},$$

$$\frac{\partial \mathbf{v}}{\partial t} = \begin{cases} \rho_s^{-1} \operatorname{div}\left(J \boldsymbol{\sigma}_s \mathbf{F}^{-T}\right) & \text{in } \Omega_s, \\ (J\rho_f)^{-1} \operatorname{div}\left(J \boldsymbol{\sigma}_f \mathbf{F}^{-T}\right) - (\nabla \mathbf{v})\mathbf{F}^{-1}(\mathbf{v} - \frac{\partial \mathbf{u}}{\partial t}) & \text{in } \Omega_f. \end{cases} \tag{1}$$

Constitutive models describing fluid and structure material properties:

$$\boldsymbol{\sigma}_f = -p_f \mathbf{I} + 2\mu_f \{\nabla \mathbf{v} \mathbf{F}^{-1}\}_s \quad \text{in } \Omega_f,$$

$$\boldsymbol{\sigma}_s = \boldsymbol{\sigma}_s(J, \mathbf{F}, p_s, \lambda_s, \mu_s, \dots) \quad \text{in } \Omega_s$$

FSI problem

Governing equations in reference subdomains

The kinematic and dynamic equations for the fluid and structure in the reference domains:

$$\frac{\partial \mathbf{u}}{\partial t} = \mathbf{v} \quad \text{in } \Omega_s,$$

$$\mathbf{G}\left(\mathbf{u}, \frac{\partial \mathbf{u}}{\partial t}\right) = 0 \quad \text{in } \Omega_f \quad \text{(extension of displacement)},$$

$$\frac{\partial \mathbf{v}}{\partial t} = \begin{cases} \rho_s^{-1} \operatorname{div}\left(J \boldsymbol{\sigma}_s \mathbf{F}^{-T}\right) & \text{in } \Omega_s, \\ (J\rho_f)^{-1} \operatorname{div}\left(J \boldsymbol{\sigma}_f \mathbf{F}^{-T}\right) - (\nabla \mathbf{v})\mathbf{F}^{-1}(\mathbf{v} - \frac{\partial \mathbf{u}}{\partial t}) & \text{in } \Omega_f. \end{cases} \tag{1}$$

Constitutive models describing fluid and structure material properties:

$$\boldsymbol{\sigma}_f = -p_f \mathbf{I} + 2\mu_f \{\nabla \mathbf{v} \mathbf{F}^{-1}\}_s \quad \text{in } \Omega_f,$$

$$\boldsymbol{\sigma}_s = \boldsymbol{\sigma}_s(J, \mathbf{F}, p_s, \lambda_s, \mu_s, \dots) \quad \text{in } \Omega_s$$

Incompressibility for fluid:

$$\operatorname{div}\left(J \mathbf{F}^{-1} \mathbf{v}\right) = J \nabla \mathbf{v} : \mathbf{F}^{-T} = 0 \quad \text{in } \Omega_f.$$

FSI problem

User-dependent equations in reference subdomains

Examples of utilized constitutive relations:

$$\boldsymbol{\sigma}_s = \frac{1}{J}\mathbf{F}(\lambda_s \mathrm{tr}(\mathbf{E})\mathbf{I} + 2\mu_s\mathbf{E})\mathbf{F}^T, \quad \text{or} \quad \boldsymbol{\sigma}_s = \mu_s\mathbf{F}\mathbf{F}^T - p_s\mathbf{I} \quad \text{in } \Omega_s.$$

FSI problem

User-dependent equations in reference subdomains

Examples of utilized constitutive relations:

$$\boldsymbol{\sigma}_s = \frac{1}{J}\mathbf{F}(\lambda_s \mathrm{tr}(\mathbf{E})\mathbf{I} + 2\mu_s \mathbf{E})\mathbf{F}^T, \quad \text{or} \quad \boldsymbol{\sigma}_s = \mu_s \mathbf{F}\mathbf{F}^T - p_s \mathbf{I} \quad \text{in } \Omega_s.$$

For incompressible version of $\boldsymbol{\sigma}_s$, we impose one of the two:

$$\begin{aligned} \operatorname{div}\left(J\mathbf{F}^{-1}\mathbf{v}\right) = J\nabla\mathbf{v} : \mathbf{F}^{-T} &= 0 \quad \text{in } \Omega_s \text{(velocity level)}, \\ J - 1 &= 0 \quad \text{in } \Omega_s \text{(displacement level)}. \end{aligned}$$

FSI problem

User-dependent equations in reference subdomains

Examples of utilized constitutive relations:

$$\boldsymbol{\sigma}_s = \frac{1}{J}\mathbf{F}(\lambda_s \mathrm{tr}(\mathbf{E})\mathbf{I} + 2\mu_s \mathbf{E})\mathbf{F}^T, \quad \text{or} \quad \boldsymbol{\sigma}_s = \mu_s \mathbf{F}\mathbf{F}^T - p_s \mathbf{I} \quad \text{in } \Omega_s.$$

For incompressible version of $\boldsymbol{\sigma}_s$, we impose one of the two:

$$\begin{aligned} \operatorname{div}(J\mathbf{F}^{-1}\mathbf{v}) = J\nabla\mathbf{v} : \mathbf{F}^{-T} &= 0 \quad \text{in } \Omega_s (\text{velocity level}), \\ J - 1 &= 0 \quad \text{in } \Omega_s (\text{displacement level}). \end{aligned}$$

Examples for extension of the displacement field to the fluid domain:

$$\begin{aligned} -\operatorname{div}(\lambda_m (\operatorname{div}\mathbf{u})\mathbf{I} + \mu_m (\nabla\mathbf{u} + \nabla\mathbf{u}^T)) &= 0 \quad \text{in } \Omega_f \\ -\Delta\mathbf{u} &= 0 \quad \text{in } \Omega_f \end{aligned}$$

FSI problem

Boundary conditions

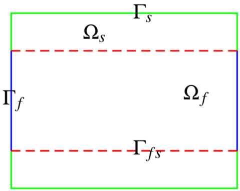

Boundary conditions:

- $\frac{\partial \mathbf{u}}{\partial t} = \mathbf{v} \quad \text{on } \Gamma_{fs},$
- $\boldsymbol{\sigma}_f \mathbf{F}^{-T}\mathbf{n} = \boldsymbol{\sigma}_s \mathbf{F}^{-T}\mathbf{n} \quad \text{on } \Gamma_{fs},$
- $\mathbf{v} = 0 \quad \text{on } \Gamma_f,$
- $\mathbf{u} = 0 \quad \text{on } \Gamma_f,$
- $\mathbf{u} = 0 \quad \text{on } \Gamma_s^0$ and $\boldsymbol{\sigma}_s \mathbf{F}^{-T}\mathbf{n} = 0 \quad \text{on } \Gamma_s^{free}.$

Numerical scheme

Conforming FE discretization with spaces $\mathbb{V}_h \subset H^1(\Omega_s \cup \Omega_f)^d$ and $\mathbb{Q}_h \subset L^2(\Omega_s \cup \Omega_f)$ satisfying LBB condition.

$$\mathbb{V}_h^0 = \{\mathbf{v} \in \mathbb{V}_h \ : \ \mathbf{v}|_{\Gamma_{fs}} = \mathbf{0}\}$$

Notation for SVK material:

$$\mathbf{E}(\mathbf{u}_1, \mathbf{u}_2) = \tfrac{1}{2}\left\{\mathbf{F}(\mathbf{u}_1)^T \mathbf{F}(\mathbf{u}_2) - \mathbf{I}\right\}_s,$$
$$\mathbf{S}(\mathbf{u}_1, \mathbf{u}_2) = \lambda_s \mathrm{tr}(\mathbf{E}(\mathbf{u}_1, \mathbf{u}_2))\mathbf{I} + 2\mu_s \mathbf{E}(\mathbf{u}_1, \mathbf{u}_2).$$

Then $\mathbf{S}(\mathbf{u}_1, \mathbf{u}_2) = \mathbf{S}^T(\mathbf{u}_1, \mathbf{u}_2) = \mathbf{S}(\mathbf{u}_2, \mathbf{u}_1)$.
Seeking solution triple $(\mathbf{u}^{k+1}, \mathbf{v}^{k+1}, p_f^{k+1}) \in \mathbb{V}_h \times \mathbb{V}_h \times \mathbb{Q}_h$ at time level $k+1$ from the following semi-implicit scheme for the case of SVK material:

Numerical scheme

$$
\begin{aligned}
&\int_{\Omega_s} \rho_s \frac{\mathbf{v}^{k+1}-\mathbf{v}^k}{\Delta t}\psi\,\mathrm{d}\mathbf{x} + \int_{\Omega_s} \mathbf{F}(\mathbf{u}^k)\mathbf{S}(\mathbf{u}^{k+1},\mathbf{u}^k) : \nabla\psi\,\mathrm{d}\mathbf{x} \\
&+ \int_{\Omega_f} \rho_f J^{k-1}\frac{\mathbf{v}^{k+1}-\mathbf{v}^k}{\Delta t}\psi\,\mathrm{d}\mathbf{x} + \int_{\Omega_f} \rho_f J^k(\nabla\mathbf{v}^{k+1})\mathbf{F}^{-1}(\mathbf{u}^k)\Big(\mathbf{v}^k - \frac{\mathbf{u}^k-\mathbf{u}^{k-1}}{\Delta t}\Big)\psi\,\mathrm{d}\mathbf{x} \\
&+ \int_{\Omega_f} 2\mu_f J^k\{(\nabla\mathbf{v}^{k+1})\mathbf{F}^{-1}(\mathbf{u}^k)\}_s : \{(\nabla\psi)\mathbf{F}^{-1}(\mathbf{u}^k)\}_s\,\mathrm{d}\mathbf{x} - \int_{\Omega_f} p_f^{k+1}J^k\mathbf{F}^{-T}(\mathbf{u}^k) : \nabla\psi\,\mathrm{d}\mathbf{x} \\
&+ \int_{\Omega_f} \frac{\rho_f}{2}\frac{J^k-J^{k-1}}{\Delta t}\mathbf{v}^{k+1}\psi + \int_{\Omega_f}\frac{\rho_f}{2}\operatorname{div}\left(J^k\mathbf{F}^{-1}(\mathbf{u}^k)\left(\mathbf{v}^k - \frac{\mathbf{u}^k-\mathbf{u}^{k-1}}{\Delta t}\right)\right)\mathbf{v}^{k+1}\psi\,\mathrm{d}\mathbf{x} \\
&+ \int_{\Omega_s} \mathbf{H}(\mathbf{u}^{k+1},\mathbf{u}^k) : \nabla\phi\,\mathrm{d}\mathbf{x} = 0 \quad \text{for all } \psi\in\mathbb{V}_h \text{ and all } \phi\in\mathbb{V}_h^0.
\end{aligned}
$$

$$
\int_{\Omega_s}\frac{\mathbf{u}^{k+1}-\mathbf{u}^k}{\Delta t}\phi\,\mathrm{d}\mathbf{x} - \int_{\Omega_s}\mathbf{v}^{k+1}\phi\,\mathrm{d}\mathbf{x} = 0 \quad \text{for all } \phi\in\mathbb{V}_h^0 \quad \text{(kinematics equation in solid)},
$$

$$
\int_{\Omega_f} J^k\nabla\mathbf{v}^{k+1} : \mathbf{F}^{-T}(\mathbf{u}^k)q\,\mathrm{d}\mathbf{x} = 0 \quad \text{for all } q\in\mathbb{Q}_h \quad \text{(incompressibility equation in fluid)}.
$$

Numerical scheme

$$
\begin{aligned}
&\int_{\Omega_s} \rho_s \frac{\mathbf{v}^{k+1}-\mathbf{v}^k}{\Delta t}\psi \,\mathrm{d}\mathbf{x} + \int_{\Omega_s} \mathbf{F}(\mathbf{u}^k)\mathbf{S}(\mathbf{u}^{k+1},\mathbf{u}^k) : \nabla\psi \,\mathrm{d}\mathbf{x} \\
&+ \int_{\Omega_f} \rho_f J^{k-1} \frac{\mathbf{v}^{k+1}-\mathbf{v}^k}{\Delta t}\psi \,\mathrm{d}\mathbf{x} + \int_{\Omega_f} \rho_f J^k (\nabla \mathbf{v}^{k+1})\mathbf{F}^{-1}(\mathbf{u}^k)\left(\mathbf{v}^k - \frac{\mathbf{u}^k-\mathbf{u}^{k-1}}{\Delta t}\right)\psi \,\mathrm{d}\mathbf{x} \\
&+ \int_{\Omega_f} 2\mu_f J^k \{(\nabla \mathbf{v}^{k+1})\mathbf{F}^{-1}(\mathbf{u}^k)\}_s : \{(\nabla\psi)\mathbf{F}^{-1}(\mathbf{u}^k)\}_s \,\mathrm{d}\mathbf{x} - \int_{\Omega_f} p_f^{k+1} J^k \mathbf{F}^{-T}(\mathbf{u}^k) : \nabla\psi \,\mathrm{d}\mathbf{x} \\
&+ \int_{\Omega_f} \frac{\rho_f}{2} \frac{J^k - J^{k-1}}{\Delta t}\mathbf{v}^{k+1}\psi + \int_{\Omega_f} \frac{\rho_f}{2} \mathrm{div}\left(J^k \mathbf{F}^{-1}(\mathbf{u}^k)\left(\mathbf{v}^k - \frac{\mathbf{u}^k-\mathbf{u}^{k-1}}{\Delta t}\right)\right)\mathbf{v}^{k+1}\psi \,\mathrm{d}\mathbf{x} \\
&+ \int_{\Omega_s} \mathbf{H}(\mathbf{u}^{k+1},\mathbf{u}^k) : \nabla\phi \,\mathrm{d}\mathbf{x} = 0 \quad \text{for all } \psi \in \mathbb{V}_h \text{ and all } \phi \in \mathbb{V}_h^0.
\end{aligned}
$$

$$
\int_{\Omega_s} \frac{\mathbf{u}^{k+1}-\mathbf{u}^k}{\Delta t}\phi \,\mathrm{d}\mathbf{x} - \int_{\Omega_s} \mathbf{v}^{k+1}\phi \,\mathrm{d}\mathbf{x} = 0 \quad \text{for all } \phi \in \mathbb{V}_h^0 \quad \text{(kinematics equation in solid)},
$$

$$
\int_{\Omega_f} J^k \nabla \mathbf{v}^{k+1} : \mathbf{F}^{-T}(\mathbf{u}^k) q \,\mathrm{d}\mathbf{x} = 0 \quad \text{for all } q \in \mathbb{Q}_h \quad \text{(incompressibility equation in fluid)}.
$$

Follows from $\frac{\partial J}{\partial t} + \mathrm{div}\,(J\mathbf{F}^{-1}(\mathbf{v} - \frac{\partial \mathbf{u}}{\partial t})) = 0$ in Ω_f.

Numerical scheme

In practice

- Higher order time-stepping is possible, such as BDF, etc. The scheme remains semi-implicit with proper extrapolation in nonlinear terms.
- Various constitutive models for solid beside SVK:
  - inc. Blatz–Ko model:

$$\mathbf{S}(\mathbf{u}_1,\mathbf{u}_2) = \mu_s(\mathtt{tr}(\{\mathbf{F}(\mathbf{u}_1)^T\mathbf{F}(\mathbf{u}_2)\}_s)\mathbf{I} - \{\mathbf{F}(\mathbf{u}_1)^T\mathbf{F}(\mathbf{u}_2)\}_s)$$

  - inc. Neo-Hookean model:

$$\mathbf{S}(\mathbf{u}_1,\mathbf{u}_2) = \mu_s\mathbf{I};\ \mathbf{F}(\mathbf{u}^k) \to \mathbf{F}(\mathbf{u}^{k+1})$$

- For incompressible solid, add $-\int_{\Omega_s} p_s^{k+1} J^k \mathbf{F}^{-T}(\mathbf{u}^k) : \nabla\psi \,\mathrm{d}\mathbf{x}$ to momentum equation and condition
  $\int_{\Omega_s} J^k \nabla\mathbf{v}^{k+1} : \mathbf{F}^{-T}(\mathbf{u}^k) q \,\mathrm{d}\mathbf{x} = 0 \quad$ for all $q \in \mathbb{Q}_h$
- Mass conservation terms are omitted in practice.

Numerical scheme

In practice

Examples of extension:

- Linear elasticity:

$$-\int_{\Omega_f} (2\mu_m \{\nabla \mathbf{u}^{k+1}\}_s : \nabla \phi + \lambda_m \mathrm{div}\, \mathbf{u}^{k+1} \mathrm{div}\, \phi)\, \mathrm{d}\mathbf{x}$$

- Harmonic:

$$-\int_{\Omega_f} \nabla \mathbf{u}^{k+1} \nabla \phi \, \mathrm{d}\mathbf{x}$$

- Heat:

$$\int_{\Omega_f} \frac{\mathbf{u}^{k+1} - \mathbf{u}^k}{\Delta t} \phi \, \mathrm{d}\mathbf{x} - \alpha \int_{\Omega_f} \nabla \mathbf{u}^{k+1} \nabla \phi \, \mathrm{d}\mathbf{x}$$

Numerical scheme

The scheme

- provides strong coupling on interface
- semi-implicit
- produces linear systems
- supports low and high order time discretizations

Numerical scheme

The scheme

- provides strong coupling on interface
- semi-implicit
- produces linear systems
- supports low and high order time discretizations
- unconditionally stable:

Theorem

Assume that the extension of the Finite Element displacement field to Ω_f is such that $J^k > 0$ for all $k = 1, \ldots, N$. Then the solution to the first order in time FE scheme shown, both for the SVK model and the incompressible neo-Hookean model, possesses a stability bound depending on the initial data.

A.Lozovskiy, M.Olshanskii, V.Salamatova, Yu.Vassilevski. An unconditionally stable semi-implicit FSI finite element method, CMAME, vol. 297, p. 437-454, 2015.

Validation in 2D: FSI3 benchmark problem

S. Turek and J. Hron. Proposal for numerical benchmarking of fluid-structure interaction between an elastic object and laminar incompressible flow. In: *Fluid-structure interaction*, Springer Berlin Heidelberg, 371–385, 2006.

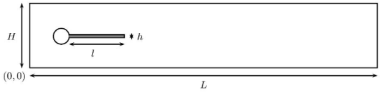

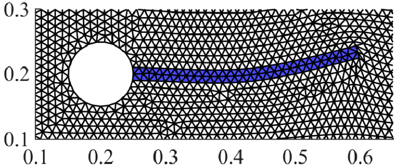

$L = 2.5,\ H = 0.41,\ l = 0.35,\ h = 0.02.$

- fluid: 2D transient Navier-Stokes, $\rho_f = 1000$, $\mu_f = 1$
- stick: SVK constitutive relation, $\rho_s = 1000$, $\lambda_s = 4\mu_s = 8 \cdot 10^6$
- outflow: "do-nothing"
- rigid walls: no-slip condition

Validation in 2D: FSI3 benchmark problem

S. Turek and J. Hron. Proposal for numerical benchmarking of fluid-structure interaction between an elastic object and laminar incompressible flow. In: *Fluid-structure interaction*, Springer Berlin Heidelberg, 371–385, 2006.

- inflow: parabolic profile

$$v_x(0, y, t) = \frac{12}{0.1681} v(t) y(H - y), \quad y \in [0, H],$$

where

$$v(t) = \begin{cases} \frac{1}{2}\left(1 - \cos\left(\frac{\pi t}{2}\right)\right) & \text{for } t < 2, \\ 1 & \text{for } t \geq 2. \end{cases}$$

- Linear elasticity extension operator for displacement in Ω_f
- Taylor-Hood element $(P_2 + P_1)$ for fluid was used.
- Grad-Div stabilization for fluid.
- Simulations were run using BDF with time step $\Delta t = 10^{-3}$ until $T = 8$.
- UMFPACK solver for linear systems

Validation in 2D: FSI3 benchmark problem

S. Turek and J. Hron. Proposal for numerical benchmarking of fluid-structure interaction between an elastic object and laminar incompressible flow. In: *Fluid-structure interaction*, Springer Berlin Heidelberg, 371–385, 2006.

Fortran open source software `Ani2D`
Advanced numerical instruments 2D, `http://sf.net/p/ani2d/`:

- mesh generation
- FEM discretization
- algebraic solvers

	# of cells in Ω_f	# of cells in Ω_s	# of DOFs
Mesh 1	8652	162	76557
Mesh 2	17540	334	154242
Mesh 3	35545	658	310997

Displacement in fluid domain:

- Harmonic $\rightarrow$ mesh tangling
- Linear elasticity with $\mu_m = \mu_s$ and $\lambda_m = \lambda_s$ $\rightarrow$ mesh tangling
- Linear elasticity with $\mu_m = 20\mu_s$ and $\lambda_m = 20\lambda_s$ for adjacent to the beam elements $\rightarrow$ OK

Validation in 2D: FSI3 benchmark problem

S. Turek and J. Hron. Proposal for numerical benchmarking of fluid-structure interaction between an elastic object and laminar incompressible flow. In: *Fluid-structure interaction*, Springer Berlin Heidelberg, 371–385, 2006.

Table: computed statistics for FSI3 test for the time interval [7,8]

Mesh/method	$u_x \cdot 10^3$	$u_y \cdot 10^3$	F_D	F_L
1	-2.8 ± 2.6	1.5 ± 34.3	432.9 ± 22.3	0.98 ± 152.1
2	-3.0 ± 2.8	1.4 ± 35.9	453.8 ± 26.8	2.6 ± 154.0
3	$\mathbf{-3.0 \pm 2.9}$	$\mathbf{1.4 \pm 36.1}$	$\mathbf{458.0 \pm 27.6}$	$\mathbf{3.0 \pm 154.5}$
Turek, S. et al	$[-3.04, -2.84]$ $\pm[2.67, 2.87]$	$[1.28, 1.55]$ $\pm[34.61, 46.63]$	$[452.4, 474.9]$ $\pm[26.19, 36.63]$	$[1.81, 3.86]$ $\pm[152.7, 165.9]$
Liu, J.	-2.91 ± 2.74	1.46 ± 35.2	460.3 ± 27.67	2.41 ± 157

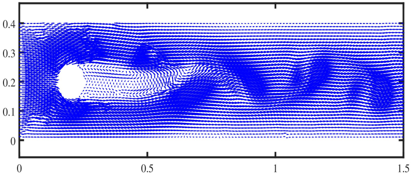

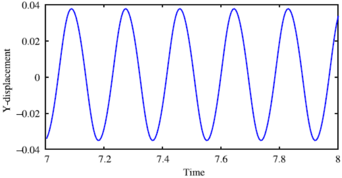

2D test: blood vessel with aneurysm

S. Turek et al. Numerical simulation and benchmarking of a monolithic multigrid solver for fluid-structure interaction problems with application to hemodynamics. In: *Fluid Structure Interaction II*, Springer Berlin Heidelberg, 193–220, 2010.

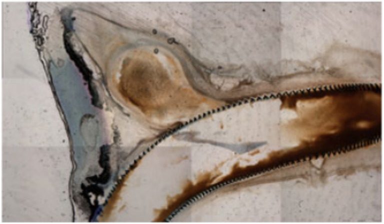

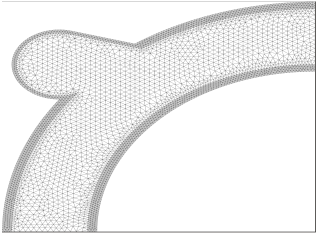

- Showing reliability of the semi-implicit scheme for hemodynamic applications
- Investigating sensitivity to compressibility of the vessel material: measuring wall shear stress(WSS) since it serves as a good indicator for the risk of aneurysm rupture

2D test: blood vessel with aneurysm

S. Turek et al. Numerical simulation and benchmarking of a monolithic multigrid solver for fluid-structure interaction problems with application to hemodynamics. In: *Fluid Structure Interaction II*, Springer Berlin Heidelberg, 193–220, 2010.

- Material properties:

ρ_s	μ_s	ρ_f	μ_f
$1.12 \cdot 10^3$ kg/m^3	270000 Pa	$1.035 \cdot 10^3$ kg/m^3	$3.4983 \cdot 10^{-3}$ Pa $\cdot$ s

- Weakly compressible neo-Hookean model:

$$\boldsymbol{\sigma}_s = \frac{\mu_s}{J^2}\left(\mathbf{FF}^T - \frac{1}{2}\mathrm{tr}\,(\mathbf{FF}^T)\mathbf{I}\right) + \left(\lambda_s + \frac{2\mu_s}{3}\right)(J-1)\mathbf{I}, \quad \lambda_s \to \infty$$

  Extrapolation is used in the model to retain semi-implicitness

- Pulsatile parabolic inflow profile:

$$v_1(0, y, t) = -50(8-y)(y-6)(1+0.75\sin(2\pi t)), \quad 6 \le y \le 8.$$

- λ_s takes on values 10^4, 10^6, 10^8 kPa, i.e. Poisson's ratio $\nu \to 0.5$.
- Global pressure made of p_s and p_f is **not** continuous along the interface Γ_{fs} in general!

2D test: blood vessel with aneurysm

S. Turek et al. Numerical simulation and benchmarking of a monolithic multigrid solver for fluid-structure interaction problems with application to hemodynamics. In: *Fluid Structure Interaction II*, Springer Berlin Heidelberg, 193–220, 2010.

WSS for weakly incompressible and fully incompressible cases, with unified and disconntected pressure:

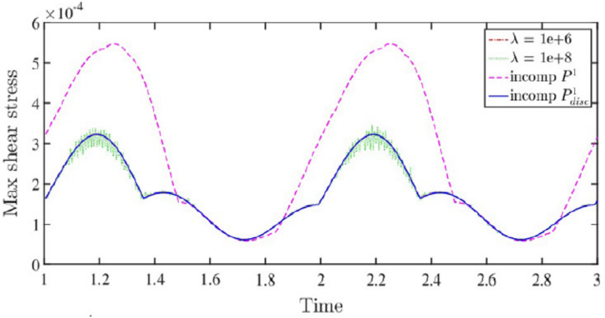

3D: silicone filament in glycerol

Benchmark challenge for CMBE 2015, Paris

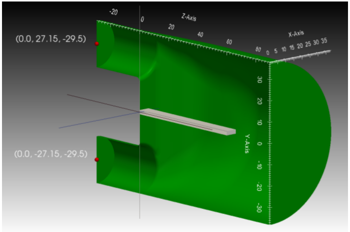

Meshed volume: original and extended domains.

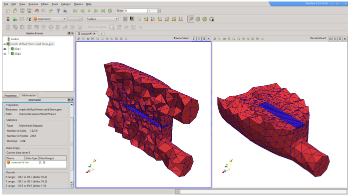

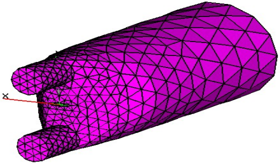

3D: silicone filament in glycerol

SVK material

M. Landajuela et al. Coupling schemes for the FSI forward prediction challenge: comparative study and validation. In: *Research Report*, RR-8824, Inria, 2015, hal-01239931v2.

- $\rho_s = 1.063 \cdot 10^{-3}$ g mm^{-3}, $\lambda_s = 140.12$ kg s^{-2}mm^{-1}, $\mu_s = 82.2$ kg s^{-2}mm^{-1}, gravity **not** neglected!
- Two inflow regimes:

	Phase I	Phase II
velocity	stationary	pulsatile
ρ_f	$1.1633 \cdot 10^{-3}$ g mm^3	$1.164 \cdot 10^{-3}$ g mm^{-3}
μ_f	$12.5 \cdot 10^{-3}$ g mm^{-1}s^{-1}	$13.37 \cdot 10^{-3}$ g mm^{-1}s^{-1}

- Inflow velocities for one cycle of frequency 1/6 Hz:

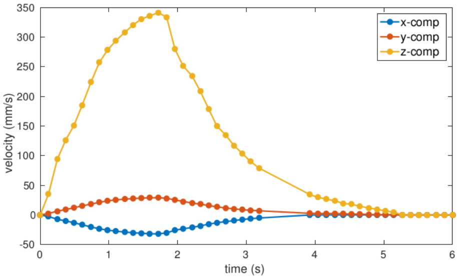

3D: silicone filament in glycerol

SVK material

M. Landajuela et al. Coupling schemes for the FSI forward prediction challenge: comparative study and validation. In: *Research Report*, RR-8824, Inria, 2015, hal-01239931v2.

- Simulation was run with $\Delta t = 10^{-2}$ s.
- The filament is lighter than the fluid and deflects upward
- Linear elasticity model is used for the **update** of the displacement extension in Ω_f! The PDE model is non-linear due to mapping to the reference domain. The Lame parameters are heterogeneous, i.e. element-volume dependent:

$$\lambda_m = 16\mu_m = 16\frac{\mu_s}{v_e^{1.2}}.$$

Software: fortran open source `ani3D`, analogous to ani2D but for... 3D. Multi-frontal massively parallel sparse direct solver (MUMPS) was used on cluster to solve the linear system at every time step.

3D: silicone filament in glycerol

SVK material

M. Landajuela et al. Coupling schemes for the FSI forward prediction challenge: comparative study and validation. In: *Research Report*, RR-8824, Inria, 2015, hal-01239931v2.

	# of cells in Ω_f	# of cells in Ω_s	# of DOFs
Mesh 1	12916	733	121104
Mesh 2	28712	733	259914
Mesh 3	51496	733	459984

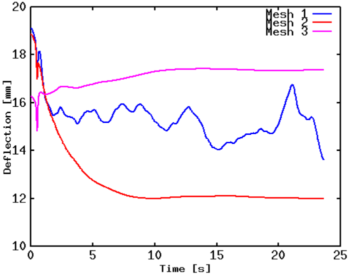

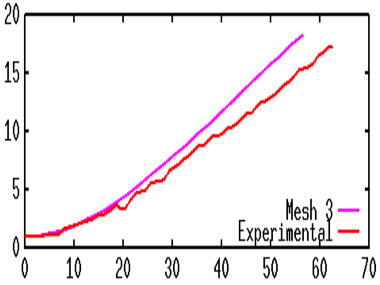

3D: silicone filament in glycerol

SVK material

M. Landajuela et al. Coupling schemes for the FSI forward prediction challenge: comparative study and validation. In: *Research Report*, RR-8824, Inria, 2015, hal-01239931v2.

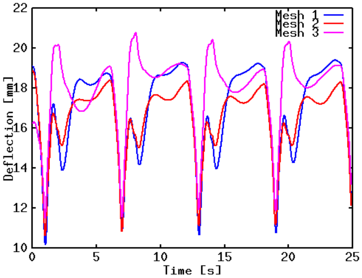

3D: silicone filament in glycerol

SVK material

M. Landajuela et al. Coupling schemes for the FSI forward prediction challenge: comparative study and validation. In: *Research Report*, RR-8824, Inria, 2015, hal-01239931v2.

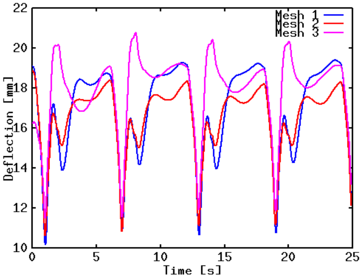

The scheme also works with incompressible neo-Hookean model. However:

- The first order semi-implicit discretization appears too dissipative: insufficiently large oscillations in phase II.
- The second-order semi-implicit BDF appears unstable even for structural tests outside of FSI

Conclusions

- We proposed unconditionally stable semi-implicit ALE FE scheme for FSI
- Only one linear system is solved per time step
- The scheme can incorporate diverse elasticity models
- Works robustly in 2D and 3D and handles various time-discretizations
- Drawback: the scheme may suffer from mesh tangling for large deformations, and the cure is ad-hoc.

Thanks for your attention!